



Published in final edited form as:

Cell Rep. 2021 January 26; 34(4): 108672. doi:10.1016/j.celrep.2020.108672.

Extracellular vesicles promote transkingdom nutrient transfer during viral-bacterial co-infection

Matthew R. Hendricks^{1,6}, Sidney Lane^{1,5}, Jeffrey A. Melvin¹, Yingshi Ouyang², Donna B. Stolz³, John V. Williams⁴, Yoel Sadovsky^{1,2}, Jennifer M. Bomberger^{1,7,*}

¹Department of Microbiology and Molecular Genetics, University of Pittsburgh School of Medicine, Pittsburgh, PA 15219, USA

²Magee-Womens Research Institute, Department of OBGYN and Reproductive Sciences, University of Pittsburgh, Pittsburgh, PA 15213, USA

³Department of Cell Biology, University of Pittsburgh School of Medicine, Pittsburgh, PA 15261, USA

⁴Department of Pediatrics, University of Pittsburgh School of Medicine, Children's Hospital of Pittsburgh of UPMC, Pittsburgh, PA 15224, USA

⁵Program in Microbiology and Immunology, University of Pittsburgh School of Medicine, Pittsburgh, PA 15219, USA

⁶Present address: Department of Immunology, University of Washington School of Medicine, Seattle, WA 98109, USA

⁷Lead contact

SUMMARY

Extracellular vesicles (EVs) are increasingly appreciated as a mechanism of communication among cells that contribute to many physiological processes. Although EVs can promote either antiviral or proviral effects during viral infections, the role of EVs in virus-associated polymicrobial infections remains poorly defined. We report that EVs secreted from airway epithelial cells during respiratory viral infection promote secondary bacterial growth, including biofilm biogenesis, by *Pseudomonas aeruginosa*. Respiratory syncytial virus (RSV) increases the release of the host iron-binding protein transferrin on the extravesicular face of EVs, which interact with *P. aeruginosa* biofilms to transfer the nutrient iron and promote bacterial biofilm growth. Vesicular delivery of iron by transferrin more efficiently promotes *P. aeruginosa* biofilm growth than soluble holo-transferrin delivered alone. Our findings indicate that EVs are a nutrient

This is an open access article under the CC BY-NC-ND license (<http://creativecommons.org/licenses/by-nc-nd/4.0/>).

*Correspondence: jbomb@pitt.edu.

AUTHOR CONTRIBUTIONS

M.R.H., J.A.M., D.B.S., J.V.W., Y.S., and J.M.B. designed experiments. M.R.H., J.A.M., S.L., and Y.O. conducted experiments. M.R.H., S.L., and J.M.B. wrote the manuscript.

DECLARATION OF INTERESTS

The authors declare no competing interests.

SUPPLEMENTAL INFORMATION

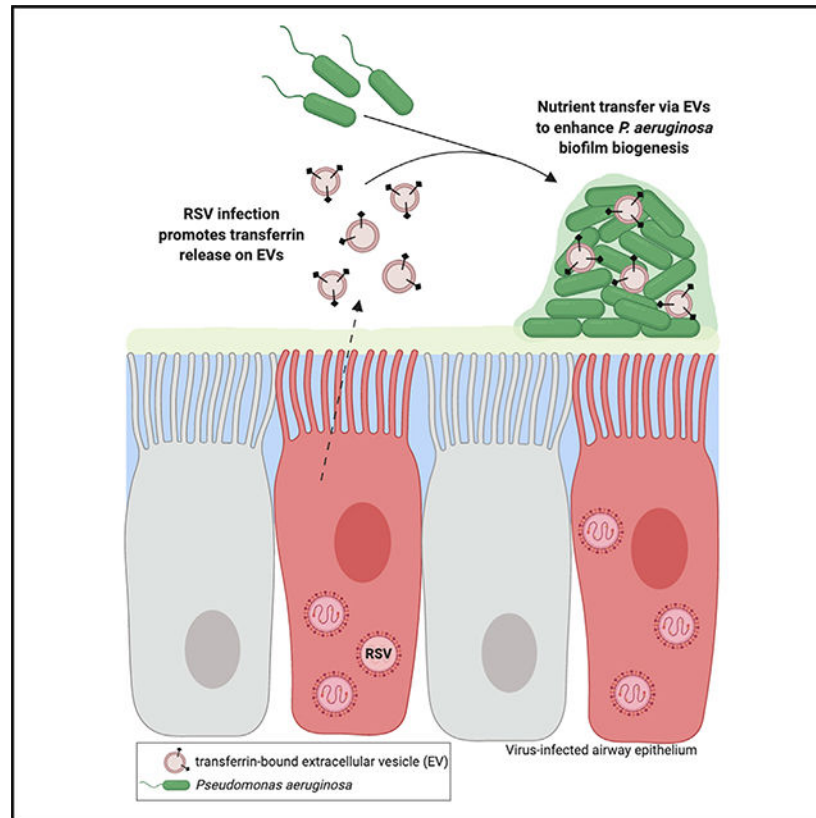
Supplemental Information can be found online at <https://doi.org/10.1016/j.celrep.2020.108672>.

source for secondary bacterial infections in the airways during viral infection and offer evidence of transkingdom communication in the setting of polymicrobial infections.

In Brief

Using cystic fibrosis as a model to study mechanisms governing viral-bacterial interactions in the lung, Hendricks et al. report that extracellular vesicles released from the respiratory epithelium during acute viral infections are a nutrient source for bacterial co-infections and offer evidence of transkingdom communication in the setting of polymicrobial infections.

Graphical Abstract



INTRODUCTION

Extracellular communication is a critical component of many host processes. Extracellular vesicles (EVs) are small, membrane-enclosed vesicles produced by most cell types and secreted into the extracellular environment. Biologically active proteins, RNAs, and lipids can be packaged into EVs and delivered to target cells, where they affect many biological processes (Lo Cicero et al., 2015). EVs derived from cells are divided into three categories: exosomes, microvesicles, and apoptotic bodies. Exosomes have been isolated from lung epithelial cells, as well as from the bronchoalveolar lavage fluid (BALF) and sputum collected from patients with chronic lung diseases, such as asthma and cystic fibrosis (CF) (Admyre et al., 2003; Kesimer et al., 2009; Moon et al., 2014; Szul et al., 2016; Torregrosa

Paredes et al., 2012). Although EVs participate in both normal tissue homeostasis and the progression of inflammation in the airways, little is known about how EVs contribute to bacterial, fungal, or viral infections in the respiratory tract (Fujita et al., 2015).

Previous work on the function of EVs during microbial infections has largely focused on functions of exosomes in the context of virus infections, where they have been reported to both promote and suppress viral infections (Raab-Traub and Dittmer, 2017). For example, replication-competent viral RNA has been observed in exosomes released by hepatitis C (HCV)-infected cells (Bukong et al., 2014; Ramakrishnaiah et al., 2013). During enterovirus 71 (EV71) infection, exosomes have also been shown to promote viral replication by suppressing antiviral immunity (Fu et al., 2017). The converse has also been reported; exosomes isolated from interferon alpha (IFN- α)-treated cells are capable of transferring IFN- α -induced antiviral immunity between cells (Li et al., 2013) and can contain microRNAs (miRNAs) that inhibit viral infection (Delorme-Axford et al., 2013). However, viral infections do not often occur in isolation, and there is an increasing appreciation for the prevalence and severity of polymicrobial infections involving viruses, yet the role EVs have in virus-associated polymicrobial infections remains unexplored.

Studies of viral-bacterial co-infections in the respiratory tract have revealed many interactions by which a preceding virus infection renders the host environment more susceptible to secondary bacterial infection. One such mechanism is by respiratory virus infections that increase bacterial adherence to host airway epithelial cells (AECs) (Avadhanula et al., 2007; Hament et al., 2005; Li et al., 2015; Novotny and Bakaletz, 2016; Smith et al., 2014; van Ewijk et al., 2008). Previous studies have also focused on how preceding respiratory viral infection subverts antibacterial immune defenses in the airways (Rynda-Apple et al., 2015). Emerging work suggests that nutritional immunity is another important process disrupted during viral-bacterial co-infections in the respiratory tract. For example, preceding influenza virus infection increases the availability of host-sialylated mucins leading to increased *Streptococcus pneumoniae* growth (Siegel et al., 2014), and we have shown that preceding respiratory syncytial virus (RSV) disrupts nutritional immunity in AECs and increases iron release from cells, which enhances *Pseudomonas aeruginosa* biofilm growth (Hendricks et al., 2016). Despite these advances, the mechanism by which nutrients are transferred between the host and pathogen during viral-bacterial co-infection is poorly understood.

To test the hypothesis that EVs mediate transkingdom communication and nutrient transfer during co-infection, we used a model of RSV-*P. aeruginosa* co-infection. *P. aeruginosa* is a commonly isolated bacterial pathogen in the lungs of patients with chronic lung disease, where it forms chronic, highly antibiotic-resistant, biofilm-associated infections (Bjarnsholt et al., 2009; Singh et al., 2000). Despite clinical studies linking respiratory viral infection with the development of bacterial infections in patients with CF (Collinson et al., 1996; Johansen and Høiby, 1992) and other chronic lung diseases, such as chronic obstructive pulmonary disease (George et al., 2014) and asthma (Kloepfer et al., 2014), very little is known about transkingdom interactions between viruses and bacteria in chronic lung diseases. Using CF lung disease as a model in the current study, we show that EVs released during virus co-infection mediate nutrient transfer between the host and *P. aeruginosa* by

interacting and promoting *P. aeruginosa* growth and transition to a biofilm lifestyle. Our results demonstrate that the release of EVs in the respiratory tract during viral infections is an important nutritional factor that dictates the outcome of polymicrobial infections.

RESULTS

EVs secreted from AECs during virus infection stimulate *P. aeruginosa* biofilm biogenesis

To examine whether EVs contribute to transkingdom interactions between bacteria and the host during viral-bacterial co-infection, we first determined whether EVs produced by uninfected and virus-infected AECs had similar molecular and physical characteristics as EVs previously isolated from the airways. Western blot analysis for standard protein markers of EVs (Figure 1A), nanoparticle tracking analysis (Figures 1B and 1C), and electron microscopy (Figure S1A) were used to confirm that the isolated EVs were of similar composition, size, and morphology as previously reported in the literature for AEC-derived EVs (Chahar et al., 2018; Kesimer et al., 2009; Moon et al., 2014; Szul et al., 2016). We next compared the growth of *P. aeruginosa* in the presence of EVs released from uninfected and virus-infected AECs. Performing growth curves in minimal media with EVs as the nutrient source, we determined that EVs from RSV-infected AECs significantly enhanced *P. aeruginosa* growth, as compared with EVs from uninfected cells (Figure 1D). To determine whether this was specific to planktonic growth or whether RSVs were also capable of enhancing *P. aeruginosa* biofilm growth, we measured *P. aeruginosa* biofilm growth in an abiotic biofilm assay. EVs from RSV-infected cells significantly increased biofilm growth, in comparison with EVs from uninfected AECs, as measured by fluorescent microscopy and 96-well microtiter biofilm assays (Figures 1E and 1F). Moreover, we observed that RSV infection increased the release of EVs from AECs, as assessed by western blot (Figure 1A) and nanoparticle tracking analysis (NTA; Figure 1C). The biofilm-stimulatory activity of EVs isolated from RSV-infected cells was dose dependent and could be diluted to levels observed with EVs isolated from uninfected AECs (Figure S1B), suggesting that increased EV release during RSV infection promotes *P. aeruginosa* biofilm growth.

The physical and chemical characteristics of EVs bear a resemblance to those of enveloped viruses, and during virus infection, diverse subpopulations of EVs are released by cells, ranging from infectious virus particles to virally induced EVs that contain viral components to EVs consisting entirely of host molecules (Nolte-'t Hoen et al., 2016). Although EVs in our study contained some RSV proteins (Figure S1D), the EV population we isolated did not contain infectious viral particles (Figure S1E). These data suggest that infectious RSV particles are not responsible for the biofilm stimulatory activity of EVs isolated from RSV-infected AECs and are consistent with our previous observations that purified RSV does not stimulate *P. aeruginosa* biofilm formation (Hendricks et al., 2016). To examine whether EV-mediated *P. aeruginosa* biofilm growth was specific to RSV infection, we isolated EVs from AECs infected with another respiratory virus commonly found in patients with CF, human rhinovirus (hRV). Interestingly, we observed that EVs isolated from hRV-infected cells also increased *P. aeruginosa* biofilm growth, although rhinovirus did not increase EV release from AECs (Figures S1F–S1H). Because EVs isolated from AECs infected with disparate viruses stimulated *P. aeruginosa* biofilm growth, we next assessed whether IFN signaling

also increases the biofilm stimulatory activity of EVs. We treated AECs with poly(I:C), which stimulates IFN production and signaling and then measured biofilm growth in the presence of EVs isolated from poly(I:C)-stimulated AECs. We found that poly(I:C) stimulates type I (IFN- β) and III (IFN- λ) production by AECs (Figure S1I), and EVs isolated from poly(I:C)-treated AECs increase *P. aeruginosa* biofilm growth (Figure S1J). Taken together, these data suggest that the innate immune response to virus infection, at least in part, mediates EV-stimulated biofilm growth.

We previously observed that the apical secretions collected from RSV-infected AECs (hereafter called “conditioned media” [CM]), contained an increased concentration of iron and were capable of enhancing *P. aeruginosa* biofilm growth (Hendricks et al., 2016). To determine whether EVs were required for CM-mediated bacterial biofilm formation, we used differential centrifugation to deplete EVs from RSV CM and measured biofilm formation. CM from RSV-infected cells that had been depleted of EVs by ultracentrifugation was unable to stimulate *P. aeruginosa* biofilm growth (Figure 1G), suggesting that EVs are required for virus-induced *P. aeruginosa* biofilm growth. Additionally, we filtered CM through 100-kDa filters, which would trap any large protein complexes or EVs but allow smaller, soluble proteins and ions to flow through. We observed that the >100-kDa fraction from RSV-infected cells maintained the ability to increase biofilm growth, similar to CM from RSV-infected cells that had not been filtered (Figure S1K). However, the <100-kDa filtrate fraction did not retain biofilm stimulatory activity (Figure S1K). These results demonstrate that EVs from RSV-infected AECs are necessary for the observed virus-stimulated bacterial growth, signifying that host-derived EVs mediate transkingdom interactions between bacteria and viruses in the airways.

EVs localize with *P. aeruginosa* biofilms

A common function of EVs is to deliver biological molecules to modify the phenotype of recipient cells. We next examined whether EVs interact with *P. aeruginosa* in biofilms. To track EV interactions with biofilms, we labeled host AECs with CellTracker Deep Red, a fluorescent dye that labels the cytoplasm of cells, as well as the lumen of released EVs (Figure S2A). Using the fluorescently labeled EVs, we examined whether EVs associated with *P. aeruginosa* biofilms in the presence or absence of virus infection. We observed association of fluorescently labeled EVs from RSV-infected cells with *P. aeruginosa* biofilms in a time-dependent manner (Figures 2A and S2C). Non-specific aggregation of labeled EVs is not observed in the absence of bacteria (Figure S2B). To further assess the interaction of host-derived EVs with *P. aeruginosa* biofilms, we examined whether host proteins can be detected in biofilms. We performed static abiotic biofilm assays with EVs, vigorously washed the bacterial biofilms, and measured EV association with *P. aeruginosa* biofilms by western blot analysis. Interestingly, we observed the presence of host vesicular proteins on biofilms (Figure 2B). These results are consistent with the conclusion that EVs from RSV-infected cells associate with *P. aeruginosa* biofilms.

To examine the mechanism by which RSV EVs stimulate *P. aeruginosa* biofilm growth, we next investigated whether EVs from RSV-infected AECs increase bacterial surface attachment. We found that there was no difference in bacterial attachment in the presence of

EVs isolated from uninfected or RSV-infected cells on either abiotic or biotic surfaces (Figures S2C and S2D). Because EVs from RSV-infected cells did not increase bacterial attachment, we hypothesized that an increased growth of surface-associated bacteria accounted for the observed, enhanced biofilm growth. To measure the effect of EVs on surface-associated growth, we allowed *P. aeruginosa* to attach to glass-bottom dishes in minimal media, washed away unattached bacteria, and then added EVs to surface-attached bacteria. We observed that surface associated bacterial growth was increased in the presence of RSV EVs, as measured by fluorescent microscopy (Figure 2C). Together, these results indicate that EVs isolated from RSV-infected AECs associate with biofilms, delivering factors, potentially, nutrients, used by *P. aeruginosa* to promote biofilm biogenesis.

RSV infection increases iron bioavailability on EVs to promote biofilm growth

Iron is required for many biological processes, including *P. aeruginosa* biofilm growth (Banin et al., 2005; Moreau-Marquis et al., 2008; Patriquin et al., 2008; Singh et al., 2002). We have previously observed that RSV infection increases extracellular iron in CM collected from AECs (Hendricks et al., 2016). However, it is not known whether iron and other metals are loaded onto EVs released by the respiratory epithelium. We observed that iron levels could be significantly reduced in CM by depleting CM of EVs by ultracentrifugation (Figure 3A), suggesting that iron is released on EVs during RSV infection. In agreement with this observation, we observed an increase in total iron on EVs isolated from RSV-infected AECs compared with control EVs (Figure 3B). This effect was specific for iron, as RSV infection did not increase other divalent metal cations, including zinc and copper (Figure 3B). RSV infection increased EV biofilm stimulatory activity and release of iron in EVs in a time-dependent manner, concurrently peaking at 72 h after RSV infection (Figure 3C). Interestingly, hRV infection and poly(I:C) treatment do not increase total iron in EVs (Figure S3A), suggesting that additional mechanisms may also govern EV-stimulated biofilm growth by *P. aeruginosa*. Importantly, in the setting of RSV co-infection, the presence of iron is necessary for EV-mediated *P. aeruginosa* biofilm growth because chelation of iron, using the chelating agent Chelex-100, significantly reduced biofilm formation in the presence of EVs from RSV-infected cells (Figure 3D). NTA was performed after Chelex-100 treatment to verify that EV abundance or morphology was not changed by iron chelation (Figure S3B).

Because RSV infection increases iron abundance in EVs and we have previously observed that RSV infection increases transferrin (Tfn) release from AECs (Hendricks et al., 2016), we next examined whether RSV infection alters the host iron-binding protein composition of EVs released by AECs. We found that RSV infection increased transferrin abundance in EVs, as assessed by western blot analysis (Figure 3E). To test the specificity of this response for transferrin, we evaluated two other iron-binding proteins, lactoferrin or ferritin, and observed that EVs from control or RSV-infected AECs did not contain these iron-binding proteins (Figure 3E). Because we observed a higher abundance of EV-associated markers in addition to transferrin (Figure 3E) during RSV infection, which is consistent with increased EV release during virus infection (Figure 1C), our results suggest that RSV infection increases production of transferrin-containing EVs during virus RSV infection. Collectively, these data suggest that RSV infection increases iron bioavailability in host-derived EVs and

EV-associated transferrin is a source of iron that promotes the formation of *P. aeruginosa* biofilms during RSV co-infection.

RSV infection increases association of transcytosed transferrin with EVs

Our data suggest a model in which virus infection releases an increased abundance of EVs loaded with transferrin into the apical compartment of cells where it is accessible to bacterial pathogens. However, transferrin is primarily a serum glycoprotein, delivered to cells by the circulatory system, which is taken up and recycled at the basolateral membrane of cells. Thus, we hypothesized that transferrin in the basolateral compartment of cells is transcytosed to the apical compartment during virus infection. We determined whether basolateral transferrin is transcytosed to the apical compartment of cells during virus infection by adding biotinylated transferrin to the basolateral media of RSV-infected cells and then used biotin affinity-purification to isolate transcytosed transferrin in apical compartment EVs (Figure 4A). We observed that significantly more biotinylated transferrin was released in association with EVs during RSV infection compared with uninfected conditions (Figure 4B). This implies that transferrin loaded onto EVs originates in the basolateral compartment. We confirmed this observation by adding fluorescein isothiocyanate (FITC)-conjugated transferrin to the basolateral compartment of AECs during RSV infection and probing EVs for FITC fluorescence (Figure S4A). Additionally, we observed that there was no transferrin associated with the biotin-negative fraction, suggesting that all transferrin localized to the EVs originated from the basolateral compartment (Figure 4B). This result is consistent with Chelex-100 treatment reducing *P. aeruginosa* biofilm growth in the presence of EVs (Figure 3D) because iron-bound transferrin loaded on the extravesicular face of EVs would be accessible to Chelex-100. In this orientation, we anticipated that biotin affinity-purification would isolate entire EVs. To test this hypothesis, we probed biotin-negative and biotin-positive fractions for EV protein markers. We demonstrated that ALIX, Tsg101, Hsp90, and MHC-I were affinity purified with biotinylated transferrin (Figure 4B), which is consistent with transferrin being receptor-bound on the outer surface of EVs. Interestingly, we observed that CD81 and flotillin-1, as well as small amounts of ALIX, Tsg101, Hsp90, and MHC-I, were present in the biotin-negative fraction (Figure 4B), indicating these proteins were not affinity purified with biotinylated transferrin. Thus, our data suggest at least two EV populations exist; one of which is transferrin positive. To investigate whether transferrin-positive EVs were necessary for biofilm biogenesis in the presence of EVs from RSV-infected AECs, we grew *P. aeruginosa* with EVs that had been depleted of transferrin-positive EVs. We found a significant decrease in *P. aeruginosa* biofilm growth in the presence of EVs when transferrin-positive EVs were removed (Figure 4C). Although we have shown that transferrin is necessary for *P. aeruginosa* biofilm growth during RSV co-infection (Hendricks et al., 2016), we observed that growing *P. aeruginosa* in levels of free transferrin, either apo- (iron-free) or holo-transferrin (iron replete), which corresponds to the levels of iron we observe in EVs (~10 μ M iron, ~5 μ M transferrin) in abiotic biofilm assays does not significantly increase *P. aeruginosa* biofilm growth (Figures 4D and S4C). This is consistent with the conclusion that the association of transferrin with EVs is important for transferrin to promote *P. aeruginosa* biofilm growth during RSV co-infection. Taken together, these data demonstrate that at least two EV populations are released by AECs and the vesicle population containing

transcytosed transferrin on the outside of EVs is necessary for *P. aeruginosa* biofilm biogenesis by RSV-stimulated EVs.

DISCUSSION

EVs are membrane-encapsulated vesicles released by most cell types into the extracellular environment where they facilitate physiological changes in neighboring cells. Although EVs have been reported in the context of viral pathogenesis to modify the local environment and regulate virus-host interactions (Raab-Traub and Dittmer, 2017), very little is understood about the role of EVs in mediating transkingdom interactions. Herein, we demonstrated that EVs released from the respiratory epithelium during respiratory viral infection enhance *P. aeruginosa* biofilm growth through a mechanism dependent upon increased release of transferrin-containing EVs. The transferrin is oriented on the extravesicular face of EVs, which makes it an accessible iron source for *P. aeruginosa* biofilm biogenesis. Moreover, we show the EVs associate with *P. aeruginosa* biofilms and that EVs loaded with iron-bound transferrin are more efficient at stimulating *P. aeruginosa* biofilm growth than iron-loaded transferrin alone. Our findings propose a role for EVs during viral-bacterial co-infections as a virally induced host nutrient source that promotes *P. aeruginosa* biofilm growth. Finally, our studies enrich our understanding of molecular mechanisms that govern the clinical observation that respiratory viral infection promotes bacterial infections in patients with chronic lung disease (Collinson et al., 1996; George et al., 2014; Johansen and Hóiby, 1992; Kloepfer et al., 2014).

Although EVs are known to be secreted into the airway lumen (Admyre et al., 2003; Fujita et al., 2015), very little is known about the biological function of EVs during respiratory infections. During virus infection in other organ systems, EVs are known to contain both antiviral and proviral mediators (Bukong et al., 2014; Delorme-Axford et al., 2013; Fu et al., 2017; Li et al., 2013; Ramakrishnaiah et al., 2013). Whether EVs affect the outcome of viral-bacterial infections or how EVs influence bacterial behavior in the airways remains unanswered questions. In our study, EVs isolated from AECs infected with disparate respiratory viruses (i.e., RSV and hRV) promote *P. aeruginosa* growth. Interestingly, RSV infection increases the apical release of EVs from AECs to promote *P. aeruginosa* biofilm growth, which is consistent with our observation that the biofilm-stimulatory activity of EVs released by RSV-infected AECs was dose dependent. The increased release of EVs from the respiratory epithelium is in line with other studies that have observed increased EV release in response to stress (i.e., infection) in other epithelial tissues (Fu et al., 2017; Hu et al., 2013; Hurwitz et al., 2017; Ramachandra et al., 2010). Our results demonstrate that EVs mediate transkingdom interactions in the respiratory tract and propose that these observations are likely to be applicable to co-infections at other mucosal sites throughout the body.

EVs commonly exert their biological effects on the local environment by delivering biological molecules to recipient cells. Although the interaction between host-derived EVs and bacteria has not been reported before, we observed that EVs derived from AECs associate with *P. aeruginosa* biofilms. The mechanism mediating EV association with *P. aeruginosa* biofilms is not understood. However, it has previously been shown that the RSV

G protein promotes association of *Haemophilus influenzae* and *S. pneumoniae* with AECs (Avadhanula et al., 2007; Smith et al., 2014). We observed that EVs isolated from RSV-infected AECs contained RSV G protein, among other host membrane proteins. Thus, it is tempting to speculate that an interaction between *P. aeruginosa* and EV membrane proteins, either host or viral, accounts for the association of EVs with biofilms. Our observations that EVs do not increase bacterial adherence to surfaces but do increase bacterial growth suggest at least one consequence of EV-bacterial interactions is that EVs provide nutrient-rich microenvironments to promote *P. aeruginosa* growth.

Studies have begun investigating how respiratory viruses alter the nutritional environment and increase nutrient availability in the airways to the benefit of bacteria (Hendricks et al., 2016; Siegel et al., 2014). It has been demonstrated that decreasing free iron levels by addition of exogenous lipocalin 2, a host iron-sequestration protein, reduces bacterial burdens in the respiratory tract during viral-bacterial co-infection (Robinson et al., 2014). Iron is required for many biological processes and is tightly regulated to limit the levels of accessible iron in the host to prevent iron intoxication and limit infections by a process termed nutritional immunity (Cassat and Skaar, 2013; Hood and Skaar, 2012). Previous studies have demonstrated the requirement of iron for *P. aeruginosa* biofilm growth (Banin et al., 2005; Moreau-Marquis et al., 2008; Patriquin et al., 2008; Singh et al., 2002), but the effect of respiratory viral infections on the nutritional environment in the airways is not well understood. We have previously shown that RSV infection dysregulates this process to promote the apical release of iron and the host iron-binding protein transferrin to stimulate *P. aeruginosa* biofilm growth (Hendricks et al., 2016), but the mechanism by which iron was released by AECs was unidentified. Here, we have extended these studies and shown that increased EV production by AECs during RSV infection is associated with increased release of transferrin-bound iron during respiratory viral co-infection. Although we cannot entirely eliminate the possibility that transferrin-bound iron is part of a macromolecular protein complex with EV marker proteins associated, we interpret our data to collectively support a model in which the transferrin-bound iron is localized on the extravesicular face of EVs, making it accessible to bacterial pathogens as well as extravesicular molecules, such as iron chelators, which can compete with bacteria for iron to prevent growth and infection.

EVs isolated from hRV-infected AECs also promoted *P. aeruginosa* biofilm growth but did not have increased iron, leading us to conclude that virus-induced EV simulation of biofilm growth is broadly observed, but different viruses change the cargo composition of EVs distinctively to facilitate transkingdom interactions during polymicrobial infections. During virus infection, EVs are also reported to influence immune cell function (Zhang et al., 2018). It is reasonable to postulate that RSV EVs may induce an altered response in immune cells that encounter EV-bound *P. aeruginosa*. Immune cells also produce EVs that have a critical role in immunomodulation (Schorey et al., 2015), although they have not been investigated regarding EV-bacterial interactions. Based on the findings detailed in this report that show host-derived AEC EVs associate with *P. aeruginosa*, it is likely that EVs from other host cells are also capable of associating with and influencing the function of bacteria. How these host-derived EV-bacterial interactions shape immune cell function during respiratory co-infection is a topic of ongoing research in the laboratory.

EVs share many physical and chemical characteristics with enveloped viruses, making separation of EVs from viruses difficult (Nolte-’t Hoen et al., 2016). Because EVs may contain viral components, this further complicates the separation of EVs that carry host proteins, viral proteins, and viral genomic elements from enveloped viruses. Thus, it is likely that diverse subpopulations of EVs are released from cells during virus infection, ranging from infectious virus particles to non-infectious, virus-induced EVs, and host EVs (Nolte-’t Hoen et al., 2016; Raab-Traub and Dittmer, 2017). Moreover, recent studies have demonstrated that defective viral genomes (DVGs) are naturally generated during virus (including influenza virus and RSV) replication and released in immunostimulatory undefined vesicle populations that fall within this spectrum (Sun et al., 2015; Tapia et al., 2013). In our study, we have shown that the EVs isolated during virus infection are not infectious, suggesting that EVs that enhance *P. aeruginosa* biofilm growth cannot be attributed to infectious virus particles. Additionally, we observed that at least two distinct subpopulations of EVs were released from AECs during RSV infection; one of which was transferrin positive. Although we cannot rule out the presence and contribution of subpopulations of non-infectious virus particles, including DVGs to *P. aeruginosa* growth, depletion of transferrin-positive EVs significantly reduced *P. aeruginosa* biofilm growth in the presence of EVs from RSV-infected cells. Thus, we conclude that this subpopulation of EVs was responsible for the biofilm stimulatory effect during RSV co-infection. Our findings collectively suggest that non-infectious, transferrin-positive EVs are responsible for enhancing *P. aeruginosa* biofilm growth and mediating transkingdom nutrient transfer during viral-bacterial co-infection.

In summary, viral-bacterial interactions result in poor bacterial clearance in patients with chronic lung disease, as well as in acute-infection settings, but the molecular mechanisms underlying these interactions and the role of EVs in these settings remain poorly understood. In this report, we demonstrate that EVs released during respiratory viral infection are used as a nutrient source for secondary bacterial infection. Our data suggest a role of EVs during respiratory viral infections that facilitate transkingdom interactions during polymicrobial infections and provide mechanistic insight into how the host contributes to the development of bacterial biofilm-associated infections during respiratory viral co-infection. Because many infectious diseases are polymicrobial and EVs are released by most cell types throughout the body, our studies likely have implications for host-pathogen interactions in many disease settings.

STAR★METHODS

RESOURCE AVAILABILITY

Lead contact—Further information and requests for resources and reagents should be directed to and will be fulfilled by the lead contact, Jennifer Bomberger (jbomb@pitt.edu).

Materials availability—This study did not generate new unique reagents.

Data and code availability—This study did not generate any unique code. Additional supplemental data have been deposited on Mendeley: <https://doi.org/10.17632/bw7c53gg8g.1>.

EXPERIMENTAL MODEL AND SUBJECT DETAILS

Cell culture—Human cells lines, bacterial strains and virus strains used in this study are listed in Key resources table. The immortalized human CF bronchial epithelial cell line CFBE41o- was cultured in minimal essential media (MEM) supplemented with 10% fetal bovine serum (FBS), 2 mM L-glutamine, 5 U/mL penicillin-5 µg/mL streptomycin (P/S) and 0.5 µg/mL Plasmocin prophylactic at 37°C in 5% CO₂. CFBE41o- were split and seeded on transwell inserts and grown at air-liquid interface in minimal essential media (MEM) supplemented with 10% fetal bovine serum (FBS), 2 mM L-glutamine, 5 U/mL penicillin-5 µg/mL streptomycin (P/S) and 0.5 µg/mL Plasmocin prophylactic for 7–10 days before use in all experiments. Cells were infected with purified human A2 strain of RSV (MOI = 1), or hRV14 (MOI = 0.1) in the apical compartment. During infections cells were cultured with MEM supplemented with 10% Exosome-depleted FBS (System Biosciences) and 2 mM L-glutamine for 72 hr in the basolateral compartment and MEM supplemented with 2 mM L-glutamine (MEM-G) in the apical compartment, unless otherwise noted.

METHOD DETAILS

Extracellular vesicle isolation—EVs were isolated from CM using differential ultracentrifugation, as described previously (Kowal et al., 2016; Théry et al., 2006). Briefly, conditioned media collected from cells was successively centrifuged at 1,400 × g for 3 min, and 10,000 × g for 30 min. Supernatants were filtered through a syringe filter unite, 0.22 µm pore size (Millipore), and then centrifuged for 90 min at 100,000 × g to pellet EVs. Pelleted EVs were resuspended in 1 mL MEM-G (10x concentration compared to conditioned media). All centrifugation steps were performed at 4°C. EV isolation was quantified using nanoparticle tracking analysis [Nanosight LM-10 (Malvern), see below for details].

Static abiotic biofilm imaging—EVs supplemented with 0.4% L-arginine were inoculated with PAO1-GFP (OD₆₀₀ normalized to 0.5) in glass-bottomed dishes (MatTek Corporation). Briefly, biofilms were grown for 6 hr at 37°C, 5% CO₂, and Z stack images of at least 10 random images were taken using a Nikon Ti-inversted microscope to measure the growth of *P. aeruginosa* biofilms (GFP, green). Nikon Elements Software version 4.60 was used to measure biofilm volume and substratum area. Biofilm biomass was calculated as the ratio of biofilm volume to substratum area.

96-Well microtiter biofilm assay—Biofilm growth on plastic microtiter dishes in the presence of CM or EVs was performed as previously described (Hendricks et al., 2016).

EV fluorescent labeling—AECs were infected with RSV for 48 hr and then stained with CellTracker Deep Red Dye (Thermo Fisher) for 45 min at 37°C. Excess dye was washed away, and EVs were isolated 24 hr later. EV fluorescence was confirmed by measuring fluorescence (Ex₆₃₀, Em₆₆₀) in a SpectraMax M2 plate reader. Media alone was used to subtract background fluorescence.

Bacterial growth curves—EVs were inoculated with overnight culture of *P. aeruginosa* strain PAO1 washed twice in MEM-G. Cultures were added to 96-well plates in quadruplicate and covered with breathable optically clear sealing membrane (Sigma). Plates

were placed in SpectraMax M2 plate reader (Molecular Devices) maintained at 37°C, and OD₆₀₀ was measured every 20 min. Media alone was used to subtract background absorbance.

Growth of pre-attached bacteria—Glass-bottomed dishes (MatTek Corporation) were inoculated with PAO1-GFP diluted in MEM (OD₆₀₀ normalized to 0.5). Unattached bacteria were gently washed away after 1 h, and biofilms were grown in the presence of EVs for 5 hr at 37°C. Z stack images of at least 10 random images were taken using a Nikon Ti inverted microscope and analyzed by Nikon Elements Software version 4.60. Biofilm biomass was calculated as the ratio of biofilm volume to substratum area.

Divalent metal measurements—Total metals were measured in EVs using QuantiChrom Iron, Copper, and Zinc Assay Kits (BioAssay Systems), respectively.

Transcytosed transferrin measurement on EVs—Transcytosed transferrin abundance on EVs was assessed as described previously with minor modifications (Tan et al., 2011). Briefly, differentiated cells were infected with RSV for 48 hr, as described above, and then the basolateral media was replaced with MEM containing phenol red supplemented with 10% EV-free FBS, 2 mM L-glutamine and 25 µg/mL transferrin biotin-XX-conjugate (Thermo Fisher). MEM-G was added to the apical compartment of cells. EVs were isolated from CM media 24 hr later, and added to Streptavidin Agarose Resin (Thermo Fisher) for 2 hr at 4°C with continuous rotation. Resin was washed twice in MEM, once in high salt solution (200 mM NaCl, 400 mM NaOAc, pH 7.4) and once more in MEM. Affinity-purified protein were eluted from resin with Laemmli Sample Buffer supplemented with dithiothreitol (DTT) and analyzed by western blot for transferrin or EV markers. Supernatants were analyzed by western blot for transferrin or EVs markers.

Depletion of transferrin containing EVs for static abiotic biofilm assays—Differentiated AECs were infected, as described above, and then the basolateral media was replaced with MEM containing phenol red supplemented with 10% EV-free FBS, 2 mM L-glutamine and 25 µg/mL transferrin biotin-XX-conjugate (Thermo Fisher) 48 hr post-infection. MEM-G was added to the apical compartment of AECs. EVs were isolated from CM media 24 hr later. EVs were added to Streptavidin Agarose Resin (Thermo Fisher) for 2 hr at 4°C with continuous rotation. Following rotation, Streptavidin Agarose Resin (including transferrin biotin-XX-conjugate containing EVs bound to resin) was pelleted from EVs at 10,000 × g for 2 min. Supernatant containing EVs (not containing transferrin biotin-XX-conjugate) was collected and used in static abiotic biofilm assays, as described above.

Western blot—Proteins were separated by SDS-PAGE on Tris gels (Bio-Rad) and were transferred onto PVDF membranes (Bio-Rad), as previously described (Bomberger et al., 2011). The following antibodies were used for protein detection: anti-ALIX (EMD Millipore), anti-calnexin (Santa Cruz Biotechnology), anti-CD81 (Thermo Fisher), anti-Flotillin-1 (BD Biosciences), anti-ferritin (Abcam), anti-GM130 (BD Biosciences), anti-Hsp90 (Enzo Life Sciences), anti-lactoferrin (Santa Cruz Biotechnology), anti-MHC-I (LifeSpan Biosciences), anti-RSV (Meridian Life Science, Inc.), anti-transferrin (Santa Cruz

Biotechnology), anti-Tsg101 (GeneTex). Secondary antibodies were goat anti-mouse, goat anti-rabbit, and rat anti-goat conjugated to HRP (Bio-Rad).

Nanoparticle tracking analysis (NTA)—EV size distribution and concentration were quantified by Nanosight LM-10 (Malvern) using a blue 405nm laser, as described previously (Ouyang et al., 2016). Briefly, EVs were diluted to an appropriate level (100- to 5,000-fold dilution) with 0.1 μ M filtered PBS (Sigma). The diluted particles were continuously injected by syringe pump into the Nanosight LM-10 view field. Particles were individually recorded and tracked for 1 min, and all frames captured were analyzed by NTA particle analysis software.

Poly(I:C) treatment—High molecular weight polyinosinic-polycytidylic acid (poly (I:C)) was floated on AECs and incubated for 72 hr, as previously described with minor modifications (Dauletbaev et al., 2015; Ioannidis et al., 2013). Differentiated AECs were treated apically with 100 μ g/mL poly (I:C) (Invivogen) and basolateral media was replaced with MEM supplemented with 10% exosome-free FBS. After a 2-hour incubation, apical media was removed. MEM-G was added to the apical compartment of cells for the final 24 hr to collect EVs.

QUANTIFICATION AND STATISTICAL ANALYSIS

Experiments were performed at least three times as indicated in the figure legends. Data are presented as mean \pm SD. GraphPad Prism version 7.0 (GraphPad) was used for statistical analysis. Means were compared using Student's t test when two datasets were compared, and for multiple comparisons, two-way ANOVA with Bonferroni's correction for multiple comparisons. $p < 0.5$ was considered significant.

Supplementary Material

Refer to Web version on PubMed Central for supplementary material.

ACKNOWLEDGMENTS

We thank Drs. Seema Lakdawala, Carolyn Coyne, and Megan Kiedrowski (University of Pittsburgh) for helpful discussion and constructive comments in the writing of this manuscript. This work was supported by the National Institutes of Health grants T32AI060525 (to M.R.H. and S.L.; PI: JoAnne L. Flynn), T32AI049820 (to J.A.M.; PI: Neal A. DeLuca), and RO1HL123771 (to J.M.B.) and the Cystic Fibrosis Foundation grants MELVIN15F0 (to J.A.M.) and BOMBER14G0 (to J.M.B.).

REFERENCES

- Admyre C, Grunewald J, Thyberg J, Gripenbäck S, Tornling G, Eklund A, Scheynius A, and Gabriellsson S (2003). Exosomes with major histocompatibility complex class II and co-stimulatory molecules are present in human BAL fluid. *Eur. Respir. J.* 22, 578–583. [PubMed: 14582906]
- Avadhanula V, Wang Y, Portner A, and Adderson E (2007). Nontypeable *Haemophilus influenzae* and *Streptococcus pneumoniae* bind respiratory syncytial virus glycoprotein. *J. Med. Microbiol.* 56, 1133–1137. [PubMed: 17761473]
- Banin E, Vasil ML, and Greenberg EP (2005). Iron and *Pseudomonas aeruginosa* biofilm formation. *Proc. Natl. Acad. Sci. USA* 102, 11076–11081. [PubMed: 16043697]

- Bjarnsholt T, Jensen PO, Fiandaca MJ, Pedersen J, Hansen CR, Andersen CB, Pressler T, Givskov M, and Høiby N (2009). *Pseudomonas aeruginosa* biofilms in the respiratory tract of cystic fibrosis patients. *Pediatr. Pulmonol.* 44, 547–558. [PubMed: 19418571]
- Bomberger JM, Ye S, Maceachran DP, Koeppen K, Barnaby RL, O’Toole GA, and Stanton BA (2011). A *Pseudomonas aeruginosa* toxin that hijacks the host ubiquitin proteolytic system. *PLoS Pathog.* 7, e1001325. [PubMed: 21455491]
- Bukong TN, Momen-Heravi F, Kodys K, Bala S, and Szabo G (2014). Exosomes from hepatitis C infected patients transmit HCV infection and contain replication competent viral RNA in complex with Ago2-miR122-HSP90. *PLoS Pathog.* 10, e1004424. [PubMed: 25275643]
- Cassat JE, and Skaar EP (2013). Iron in infection and immunity. *Cell Host Microbe* 13, 509–519. [PubMed: 23684303]
- Chahar HS, Corsello T, Kudlicki AS, Komaravelli N, and Casola A (2018). Respiratory syncytial virus infection changes cargo composition of exosome released from airway epithelial cells. *Sci. Rep.* 8, 387. [PubMed: 29321591]
- Collinson J, Nicholson KG, Cancio E, Ashman J, Ireland DC, Hammersley V, Kent J, and O’Callaghan C (1996). Effects of upper respiratory tract infections in patients with cystic fibrosis. *Thorax* 51, 1115–1122. [PubMed: 8958895]
- Dauletbaev N, Cammisano M, Herscovitch K, and Lands LC (2015). Stimulation of the RIG-I/MAVS pathway by polyinosinic:polycytidylic acid upregulates IFN- β in airway epithelial cells with minimal costimulation of IL-8. *J. Immunol.* 195, 2829–2841. [PubMed: 26283481]
- Delorme-Axford E, Donker RB, Mouillet JF, Chu T, Bayer A, Ouyang Y, Wang T, Stolz DB, Sarkar SN, Morelli AE, et al. (2013). Human placental trophoblasts confer viral resistance to recipient cells. *Proc. Natl. Acad. Sci. USA* 110, 12048–12053. [PubMed: 23818581]
- Fu Y, Zhang L, Zhang F, Tang T, Zhou Q, Feng C, Jin Y, and Wu Z (2017). Exosome-mediated miR-146a transfer suppresses type I interferon response and facilitates EV71 infection. *PLoS Pathog.* 13, e1006611. [PubMed: 28910400]
- Fujita Y, Kosaka N, Araya J, Kuwano K, and Ochiya T (2015). Extracellular vesicles in lung microenvironment and pathogenesis. *Trends Mol. Med.* 21, 533–542. [PubMed: 26231094]
- George SN, Garcha DS, Mackay AJ, Patel AR, Singh R, Sapsford RJ, Donaldson GC, and Wedzicha JA (2014). Human rhinovirus infection during naturally occurring COPD exacerbations. *Eur. Respir. J.* 44, 87–96. [PubMed: 24627537]
- Hament JM, Aerts PC, Fleer A, van Dijk H, Harmsen T, Kimpen JL, and Wolfs TF (2005). Direct binding of respiratory syncytial virus to pneumococci: a phenomenon that enhances both pneumococcal adherence to human epithelial cells and pneumococcal invasiveness in a murine model. *Pediatr. Res.* 58, 1198–1203. [PubMed: 16306193]
- Hendricks MR, Lashua LP, Fischer DK, Flitter BA, Eichinger KM, Durbin JE, Sarkar SN, Coyne CB, Empey KM, and Bomberger JM (2016). Respiratory syncytial virus infection enhances *Pseudomonas aeruginosa* biofilm growth through dysregulation of nutritional immunity. *Proc. Natl. Acad. Sci. USA* 113, 1642–1647. [PubMed: 26729873]
- Hood MI, and Skaar EP (2012). Nutritional immunity: transition metals at the pathogen-host interface. *Nat. Rev. Microbiol.* 10, 525–537. [PubMed: 22796883]
- Hu G, Gong AY, Roth AL, Huang BQ, Ward HD, Zhu G, Larusso NF, Hanson ND, and Chen XM (2013). Release of luminal exosomes contributes to TLR4-mediated epithelial antimicrobial defense. *PLoS Pathog.* 9, e1003261. [PubMed: 23592986]
- Hurwitz SN, Nkosi D, Conlon MM, York SB, Liu X, Tremblay DC, and Meckes DG Jr. (2017). CD63 regulates Epstein-Barr virus LMP1 exosomal packaging, enhancement of vesicle production, and noncanonical NF- κ B signaling. *J. Virol.* 91, e02251–16. [PubMed: 27974566]
- Ioannidis I, Ye F, McNally B, Willette M, and Flaño E (2013). Toll-like receptor expression and induction of type I and type III interferons in primary airway epithelial cells. *J. Virol.* 87, 3261–3270. [PubMed: 23302870]
- Johansen HK, and Høiby N (1992). Seasonal onset of initial colonisation and chronic infection with *Pseudomonas aeruginosa* in patients with cystic fibrosis in Denmark. *Thorax* 47, 109–111. [PubMed: 1549817]

- Kesimer M, Scull M, Brighton B, DeMaria G, Burns K, O'Neal W, Pickles RJ, and Sheehan JK (2009). Characterization of exosome-like vesicles released from human tracheobronchial ciliated epithelium: a possible role in innate defense. *FASEB J.* 23, 1858–1868. [PubMed: 19190083]
- Kloepfer KM, Lee WM, Pappas TE, Kang TJ, Vrtis RF, Evans MD, Gangnon RE, Bochkov YA, Jackson DJ, Lemanske RF Jr., et al. (2014). Detection of pathogenic bacteria during rhinovirus infection is associated with increased respiratory symptoms and asthma exacerbations. *J. Allergy Clin. Immunol.* 133, 1301–1307. [PubMed: 24698319]
- Kowal J, Arras G, Colombo M, Jouve M, Morath JP, Primdal-Bengtson B, Dingli F, Loew D, Tkach M, and Théry C (2016). Proteomic comparison defines novel markers to characterize heterogeneous populations of extracellular vesicle subtypes. *Proc. Natl. Acad. Sci. USA* 113, E968–E977. [PubMed: 26858453]
- Kuchma SL, Connolly JP, and O'Toole GA (2005). A three-component regulatory system regulates biofilm maturation and type III secretion in *Pseudomonas aeruginosa*. *J. Bacteriol.* 187, 1441–1454. [PubMed: 15687209]
- Li J, Liu K, Liu Y, Xu Y, Zhang F, Yang H, Liu J, Pan T, Chen J, Wu M, et al. (2013). Exosomes mediate the cell-to-cell transmission of IFN- α -induced antiviral activity. *Nat. Immunol.* 14, 793–803. [PubMed: 23832071]
- Li N, Ren A, Wang X, Fan X, Zhao Y, Gao GF, Cleary P, and Wang B (2015). Influenza viral neuraminidase primes bacterial coinfection through TGF- β -mediated expression of host cell receptors. *Proc. Natl. Acad. Sci. USA* 112, 238–243. [PubMed: 25535343]
- Lo Cicero A, Stahl PD, and Raposo G (2015). Extracellular vesicles shuffling intercellular messages: for good or for bad. *Curr. Opin. Cell Biol.* 35, 69–77. [PubMed: 26001269]
- Moon HG, Kim SH, Gao J, Quan T, Qin Z, Osorio JC, Rosas IO, Wu M, Tesfaigzi Y, and Jin Y (2014). CCN1 secretion and cleavage regulate the lung epithelial cell functions after cigarette smoke. *Am. J. Physiol. Lung Cell. Mol. Physiol.* 307, L326–L337. [PubMed: 24973403]
- Moreau-Marquis S, Bomberger JM, Anderson GG, Swiatecka-Urban A, Ye S, O'Toole GA, and Stanton BA (2008). The DeltaF508-CFTR mutation results in increased biofilm formation by *Pseudomonas aeruginosa* by increasing iron availability. *Am. J. Physiol. Lung Cell. Mol. Physiol.* 295, L25–L37. [PubMed: 18359885]
- Nolte-t Hoen E, Cremer T, Gallo RC, and Margolis LB (2016). Extracellular vesicles and viruses: are they close relatives? *Proc. Natl. Acad. Sci. USA* 113, 9155–9161. [PubMed: 27432966]
- Novotny LA, and Bakaletz LO (2016). Intercellular adhesion molecule 1 serves as a primary cognate receptor for the type IV pilus of nontypeable *Haemophilus influenzae*. *Cell. Microbiol.* 18, 1043–1055. [PubMed: 26857242]
- Ouyang Y, Bayer A, Chu T, Tyurin VA, Kagan VE, Morelli AE, Coyne CB, and Sadovsky Y (2016). Isolation of human trophoblastic extracellular vesicles and characterization of their cargo and antiviral activity. *Placenta* 47, 86–95. [PubMed: 27780544]
- Patriquin GM, Banin E, Gilmour C, Tuchman R, Greenberg EP, and Poole K (2008). Influence of quorum sensing and iron on twitching motility and biofilm formation in *Pseudomonas aeruginosa*. *J. Bacteriol.* 190, 662–671. [PubMed: 17993517]
- Raab-Traub N, and Dittmer DP (2017). Viral effects on the content and function of extracellular vesicles. *Nat. Rev. Microbiol.* 15, 559–572. [PubMed: 28649136]
- Ramachandra L, Qu Y, Wang Y, Lewis CJ, Cobb BA, Takatsu K, Boom WH, Dubyak GR, and Harding CV (2010). *Mycobacterium tuberculosis* synergizes with ATP to induce release of microvesicles and exosomes containing major histocompatibility complex class II molecules capable of antigen presentation. *Infect. Immun.* 78, 5116–5125. [PubMed: 20837713]
- Ramakrishnaiah V, Thumann C, Fofana I, Habersetzer F, Pan Q, de Ruyter PE, Willemsen R, Demmers JA, Stalin Raj V, Jenster G, et al. (2013). Exosome-mediated transmission of hepatitis C virus between human hepatoma Huh7.5 cells. *Proc. Natl. Acad. Sci. USA* 110, 13109–13113. [PubMed: 23878230]
- Robinson KM, McHugh KJ, Mandalapu S, Clay ME, Lee B, Scheller EV, Enelow RI, Chan YR, Kolls JK, and Alcorn JF (2014). Influenza A virus exacerbates *Staphylococcus aureus* pneumonia in mice by attenuating antimicrobial peptide production. *J. Infect. Dis.* 209, 865–875. [PubMed: 24072844]

- Rynda-Apple A, Robinson KM, and Alcorn JF (2015). Influenza and bacterial superinfection: illuminating the immunologic mechanisms of disease. *Infect. Immun.* 83, 3764–3770. [PubMed: 26216421]
- Schorey JS, Cheng Y, Singh PP, and Smith VL (2015). Exosomes and other extracellular vesicles in host-pathogen interactions. *EMBO Rep* 16, 24–43. [PubMed: 25488940]
- Siegel SJ, Roche AM, and Weiser JN (2014). Influenza promotes pneumococcal growth during coinfection by providing host sialylated substrates as a nutrient source. *Cell Host Microbe* 16, 55–67. [PubMed: 25011108]
- Singh PK, Schaefer AL, Parsek MR, Moninger TO, Welsh MJ, and Greenberg EP (2000). Quorum-sensing signals indicate that cystic fibrosis lungs are infected with bacterial biofilms. *Nature* 407, 762–764. [PubMed: 11048725]
- Singh PK, Parsek MR, Greenberg EP, and Welsh MJ (2002). A component of innate immunity prevents bacterial biofilm development. *Nature* 417, 552–555. [PubMed: 12037568]
- Smith CM, Sandrini S, Datta S, Freestone P, Shafeeq S, Radhakrishnan P, Williams G, Glenn SM, Kuipers OP, Hirst RA, et al. (2014). Respiratory syncytial virus increases the virulence of *Streptococcus pneumoniae* by binding to penicillin binding protein 1a: a new paradigm in respiratory infection. *Am. J. Respir. Crit. Care Med.* 190, 196–207. [PubMed: 24941423]
- Sun Y, Jain D, Koziol-White CJ, Genoyer E, Gilbert M, Tapia K, Panettieri RA Jr., Hodinka RL, and López CB (2015). Immunostimulatory defective viral genomes from respiratory syncytial virus promote a strong innate antiviral response during infection in mice and humans. *PLoS Pathog.* 11, e1005122. [PubMed: 26336095]
- Szul T, Bratcher PE, Fraser KB, Kong M, Tirouvanziam R, Ingersoll S, Sztul E, Rangarajan S, Blalock JE, Xu X, and Gaggar A (2016). Toll-like receptor 4 engagement mediates prolyl endopeptidase release from airway epithelia via exosomes. *Am. J. Respir. Cell Mol. Biol.* 54, 359–369. [PubMed: 26222144]
- Tan S, Noto JM, Romero-Gallo J, Peek RM Jr., and Amieva MR (2011). *Helicobacter pylori* perturbs iron trafficking in the epithelium to grow on the cell surface. *PLoS Pathog.* 7, e1002050. [PubMed: 21589900]
- Tapia K, Kim WK, Sun Y, Mercado-López X, Dunay E, Wise M, Adu M, and López CB (2013). Defective viral genomes arising in vivo provide critical danger signals for the triggering of lung antiviral immunity. *PLoS Pathog.* 9, e1003703. [PubMed: 24204261]
- Théry C, Amigorena S, Raposo G, and Clayton A (2006). Isolation and characterization of exosomes from cell culture supernatants and biological fluids. *Curr. Protoc. Cell Biol.* Chapter 3, Unit 3.22.
- Torregrosa Paredes P, Esser J, Admyre C, Nord M, Rahman QK, Lukic A, Rådmark O, Grönneberg R, Grunewald J, Eklund A, et al. (2012). Bronchoalveolar lavage fluid exosomes contribute to cytokine and leukotriene production in allergic asthma. *Allergy* 67, 911–919. [PubMed: 22620679]
- van Ewijk BE, van der Zalm MM, Wolfs TF, Fleer A, Kimpfen JL, Wilbrink B, and van der Ent CK (2008). Prevalence and impact of respiratory viral infections in young children with cystic fibrosis: prospective cohort study. *Pediatrics* 122, 1171–1176. [PubMed: 19047230]
- Zhang W, Jiang X, Bao J, Wang Y, Liu H, and Tang L (2018). Exosomes in pathogen infections: a bridge to deliver molecules and link functions. *Front. Immunol.* 9, 90. [PubMed: 29483904]

Highlights

- Extracellular vesicles (EVs) associate with *Pseudomonas aeruginosa* biofilms
- EVs secreted from virus-infected respiratory epithelia promote *P. aeruginosa* biofilm
- RSV infection increases transcytosed transferrin and iron on EVs to promote biofilm
- EVs are a nutrient source that mediate host-pathogen interactions in the lung

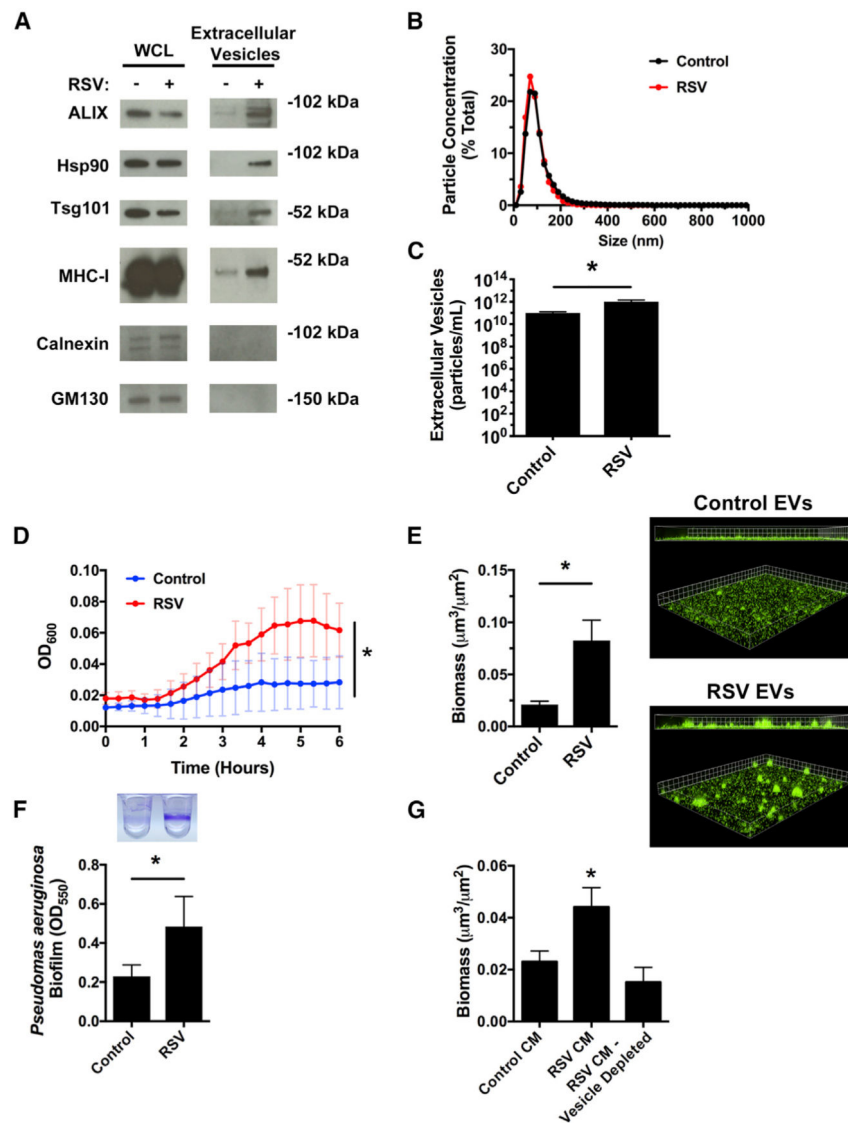


Figure 1. EVs from RSV-infected cells increase *P. aeruginosa* planktonic and biofilm growth AECs were infected with RSV or mock infected (MEM control) for 72 h, and EVs were isolated from the apical secretions of cells.

(A and B) RSV infection increases EV secretion from AECs.

(A) EVs were characterized by western blot analysis for standard protein markers of EVs.

(B) RSV infection does not alter the size distribution of EVs released by AECs as analyzed by nanoparticle tracking analysis (NTA). Histogram displaying the size distribution of purified EVs.

(C) RSV infection increases EV release from AECs. EV concentration was analyzed by NTA.

(D) Bacterial growth curves were performed to measure planktonic growth of *P. aeruginosa* in the presence of EVs collected from AECs.

(E) *P. aeruginosa* (GFP, green) was grown in the presence of EVs in static abiotic biofilm assays (grid unit = 8 µM).

(F) *P. aeruginosa* biofilms were grown in the presence of EVs in 96-well microtiter biofilm assays.

(G) AECs were infected with RSV or mock infected (MEM control) for 72 h and apical CM was collected. CM was depleted of EVs by ultracentrifugation, and *P. aeruginosa* biofilms were grown in static abiotic biofilm assays.

Control, EVs from mock-infected AECs; RSV, EVs from RSV-infected AECs. For all experiments, n = 3. Data are presented as means ± SD. *p < 0.05 versus control.

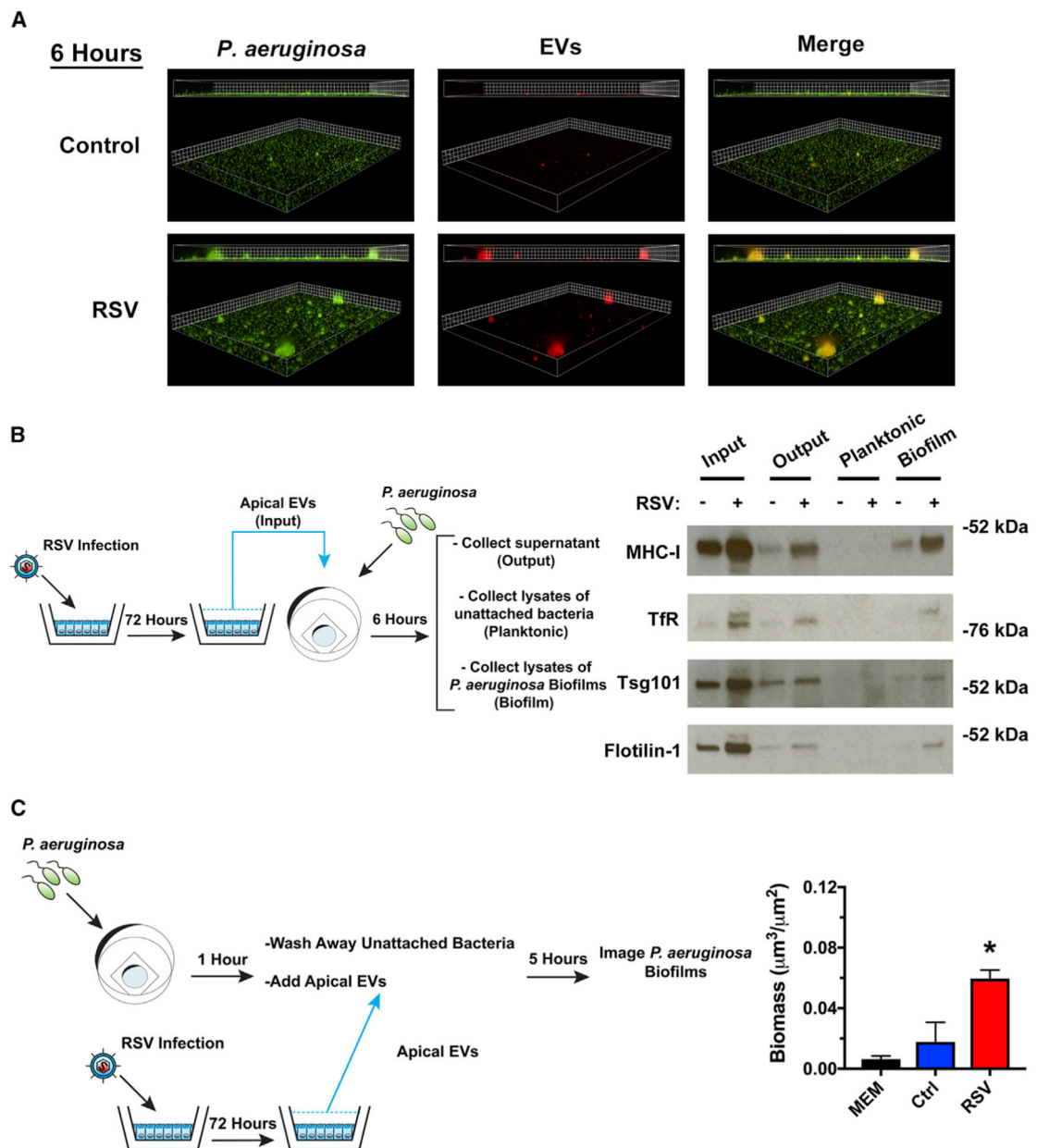


Figure 2. RSV EVs localize with *P. aeruginosa* biofilms and increase growth of surface-associated *P. aeruginosa*

(A) EVs isolated from RSV-infected AECs associate with *P. aeruginosa* biofilms. AECs were infected with RSV or were mock infected (MEM control) for 48 h. Cells were labeled with CellTracker Deep Red Dye for 45 min, and EVs were collected from dye-labeled cells 24 h later. *P. aeruginosa* (GFP, green) was grown in the presence of EVs (CellTracker Deep Red, red) for 6 h in static abiotic biofilm assays (grid unit = 5 μM).

(B and C) EVs were isolated from AECs infected with RSV or mock infected (MEM control) for 72 h.

(B) EVs associate with surface associated biofilms in static abiotic biofilm assays, as measured by western blot analysis. EV protein abundance was assessed in (1) EVs before

(input) static abiotic biofilm assays, (2) EVs collected after (output) static abiotic biofilm assays, (3) planktonic bacteria collected off the top of static abiotic biofilm assays and washed 2× (planktonic), and (4) in surface-associated bacteria washed 2× (biofilm). The schematic outlines experimental design and the fractions analyzed by western blot analysis. (C) EVs from RSV-infected AECs increase the growth of surface associated *P. aeruginosa*. Schematic outlines experimental design. Briefly, *P. aeruginosa* was given 1 h to attach to glass-bottom dishes. Surface-associated bacteria were grown in the presence of EVs for 5 h in static abiotic biofilm assays. Control, EVs from mock-infected AECs; RSV, EVs from RSV-infected AECs. For all experiments, n = 3. Data are presented as means ± SD. *p < 0.05 versus control.

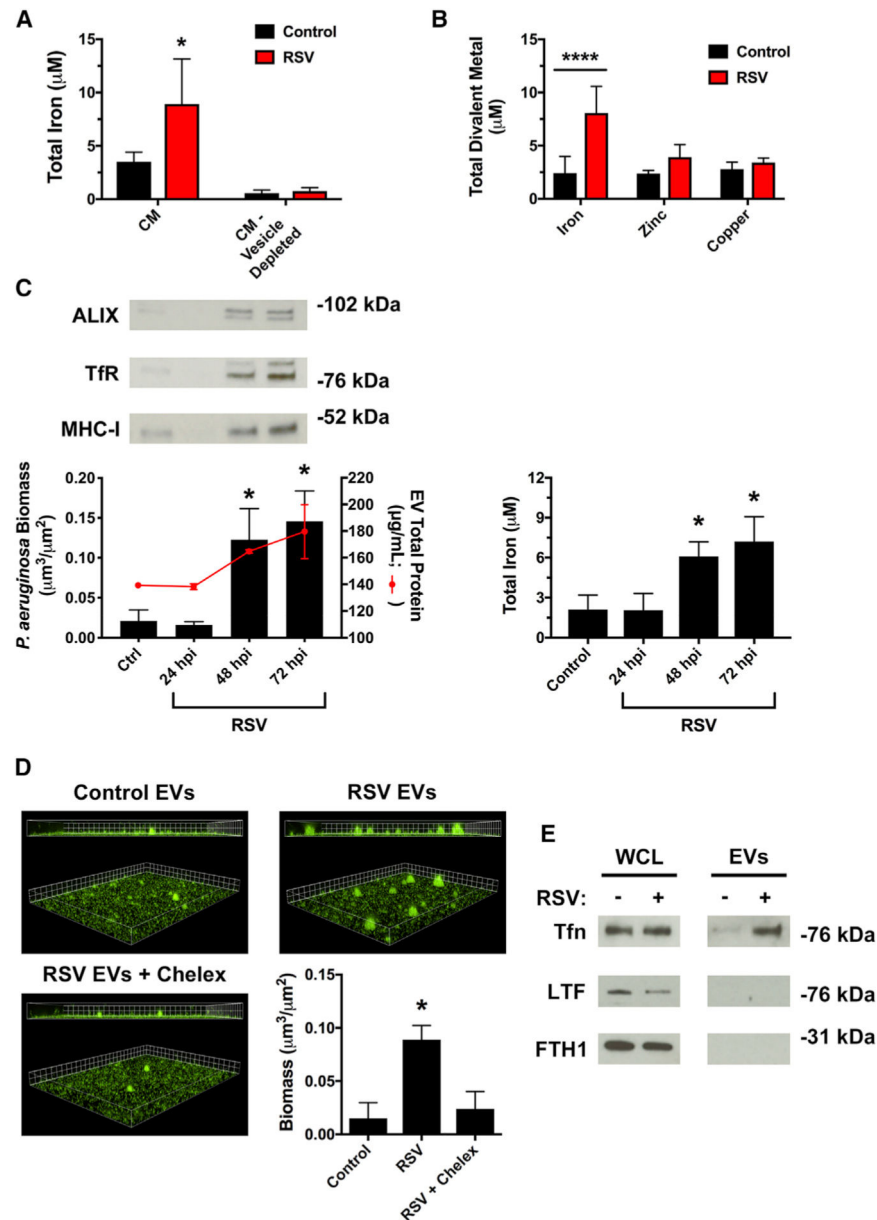


Figure 3. RSV infection increases iron associated with EVs to stimulate biofilm growth
 (A and B) RSV infection increases iron association with EVs. Cells were infected with RSV or mock-infected (MEM control) for 72 h. The abundance of divalent metals was measured in (A) CM and CM depleted of EVs by ultracentrifugation or (B) EVs.
 (C) *P. aeruginosa* (GFP) was grown in static abiotic biofilm assays in the presence of EVs isolated from AECs infected with RSV for the indicated number of hours. Protein and total iron were analyzed in EVs isolated at the indicated hours post RSV infection (hpi).
 (D) Iron in EVs is required for the growth of *P. aeruginosa* biofilms. EVs were isolated from AECs infected with RSV or mock infected (MEM control) for 72 h, and static abiotic biofilm assays were performed to measure *P. aeruginosa* (GFP) biofilms (grid unit = 8 µM). Divalent metal cations were chelated with Chelex-100 resin (labeled “Chelex”) for 1 h.

Chelex-100 was removed from EVs by centrifugation at $11,000 \times g$ for 3 min prior to biofilm assays.

(E) RSV infection increases transferrin abundance in EVs, as measured by western blot analysis.

Tfn, transferrin; LTF, lactoferrin; FTH1, ferritin. Control, EVs from mock-infected AECs; RSV, EVs from RSV-infected AECs. For all experiments, $n = 3$. Data are presented as means \pm SD. * $p < 0.05$ versus control.

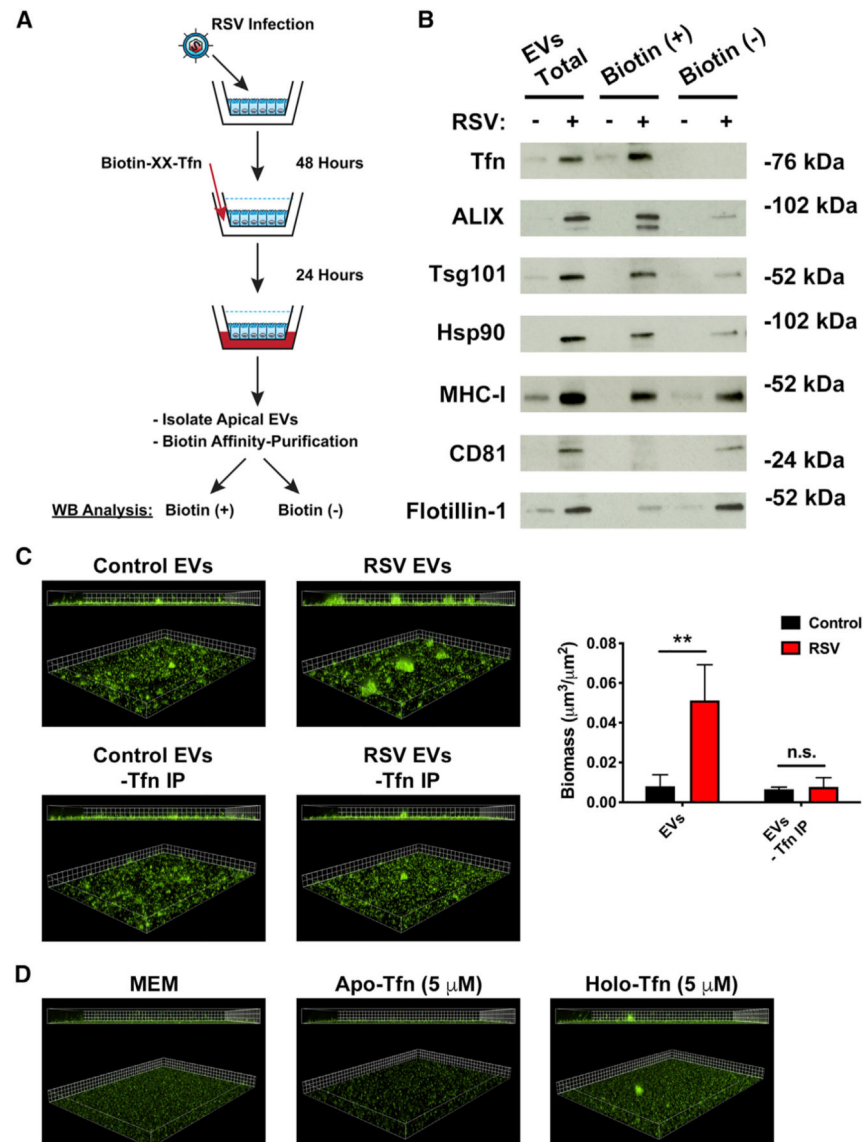


Figure 4. Transcytosed transferrin is loaded on the outside of EVs to enhance *P. aeruginosa* biofilm growth during RSV infection

AECs were infected with RSV or mock infected (MEM control) for 48 h. Biotinylated-transferrin was added to the basolateral chamber of RSV or mock-infected AECs at a final concentration of 25 $\mu\text{g}/\text{mL}$. EVs were collected from the apical CM of AECs 24 h later, and biotinylated-transferrin was affinity purified from EV preparations with streptavidin-coated beads. Bead-bound proteins were eluted from the resin (transferrin IP), and supernatant from the streptavidin resin (IP Sup) were separated by SDS-PAGE.

(A) Schematic of experimental design.

(B) Transcytosed transferrin and protein markers of EVs were measured by western blot analysis in transferrin IP (biotin-positive) and IP Sup (biotin-negative) fractions.

(C) *P. aeruginosa* (GFP) was grown in the presence of EVs in static abiotic biofilm assays after biotin affinity purification to remove transferrin-positive EVs (grid unit = 7.5 μm).

(D) Free, EV-unbound transferrin sources (apo- and holo-transferrin; iron-free and iron-replete, respectively) dissolved in MEM do not promote *P. aeruginosa* (GFP, green) biofilm growth. Biofilm growth was measured by static abiotic biofilm assays (grid unit = 7.5 μm). Control, EVs from mock-infected AECs; RSV, EVs from RSV-infected AECs. For all experiments $n = 3$. Data are presented as means \pm SD. * $p < 0.05$ versus control.

Author Manuscript

Author Manuscript

Author Manuscript

Author Manuscript

KEY RESOURCES TABLE

REAGENT or RESOURCE	SOURCE	IDENTIFIER
Antibodies		
ALIX	EMD Millipore	Cat. # ABC40; RRID: AB_10806218
Calnexin	Santa Cruz Biotechnology	Cat. # sc-70481; RRID: AB_1119917
CD81	Thermo Fisher	Cat. # PA5-13582; RRID: AB_2076269
Ferritin	Abcam	Cat. # ab75972; RRID: AB_1310223
Flotillin-1	BD Biosciences	Cat. # 610820; RRID: AB_398139
GM130	BD Biosciences	Cat. # 610822; RRID: AB_398141
Hsp90	Enzo Life Sciences	Cat. # ADI-SPA-830; RRID: AB_10616102
Lactoferrin	Santa Cruz Biotechnology	Cat. # sc-25622; RRID: AB_2139339
MHC-I	LifeSpan Biosciences	Cat. # LS-C107394; RRID: AB_10627058
RSV	Meridian Life Sciences, Inc.	Cat. # B65840G; RRID: AB_152744
Transferrin	Santa Cruz Biotechnology	Cat. # sc-52256; RRID: AB_630356
Tsg101	GeneTex	Cat. # GTX70255; RRID: AB_373239
Goat Anti-Mouse IgG (HRP-Conjugated)	Bio-Rad	Cat. # 172-1011; RRID: AB_11125936
Goat Anti-Rabbit IgG (HRP-Conjugated)	Bio-Rad	Cat. # 172-1019; RRID: AB_11125143
Rat Anti-Goat IgG (HRP-Conjugated)	Santa Cruz Biotechnology	Cat. # sc-2020; RRID: AB_631728
Bacterial and virus strains		
<i>Pseudomonas aeruginosa</i> PAO1-GFP [constitutively expresses <i>gfp</i> (pSMC21)]	Lab Stock	N/A
Respiratory Syncytial Virus A2	Lab Stock	N/A
Human Rhinovirus 14	Lab Stock	N/A
Chemicals, peptides, and recombinant proteins		
CellTracker Deep Red Dye	Thermo Fisher	Cat. # C34565
Poly(I:C)	InvivoGen	Cat. #tlrl-pic
Streptavidin Agarose Resin	Thermo Fisher	Cat. # 20349
Transferrin Biotin-XX-Conjugate	Thermo Fisher	Cat. # T23363
Transferrin Fluorescein Conjugate	Thermo Fisher	Cat. # T2871
Critical commercial assays		
Human IFN-beta DuoSet ELISA	R&D Systems	Cat. # DY814-05
Human IL-29/IL-28B (IFN-lambda 1/3) DuoSet ELISA	R&D Systems	Cat. # DY1598B
QuantiChrom Copper Assay Kit	BioAssay Systems	Cat. # DICU-250
QuantiChrom Iron Assay Kit	BioAssay Systems	Cat. # DIFE-250
QuantiChrom Zinc Assay Kit	BioAssay Systems	Cat. # DIZN-250
Deposited data		
Mendeley data – additional supplemental data	This Paper	

REAGENT or RESOURCE	SOURCE	IDENTIFIER
Experimental models: cell lines		
Human: CFBE41o-	Laboratory of John P. Clancy	N/A
Recombinant DNA		
pSMC21	Kuchma et al., 2005	N/A
Software and algorithms		
GraphPad Prism 7	GraphPad	RRID: SCR_002798; https://www.graphpad.com/scientific-software/prism/
NanoSight NTA 3.2	Malvern Panalytical	RRID: SCR_014239; https://www.malvernpanalytical.com/en/products/technology/light-scattering/nanoparticle-tracking-analysis
Nikon Elements version v4.60	Nikon Instruments	RRID: SCR_014329; https://www.microscope.healthcare.nikon.com/products/software/nis-elements
Other		
35 mm Glass-Bottom Dish	MatTek Corporation	Cat. # P35G-1.0-14-C
4x Laemmli Sample Buffer	Bio-Rad	Cat. # 1610747
96-well Microtiter Dishes	Fisher Scientific	Cat. # 07-200-99
96-well Microtiter Dish Lids	Fisher Scientific	Cat. # 14-245-63A
96-well Plates – Bacterial Growth Curves	Fisher Scientific	Cat. # 08-772-53
Breathe-Easy® Sealing Membrane	Sigma Aldrich	Cat. # Z380059
Corning Costar 75 mm Transwell Inserts	Fisher Scientific	Cat. # 07-200-172
Exosome-Depleted FBS	Fisher Scientific	Cat. # NC0464480
L-arginine	Fisher Scientific	Cat. # BP370-100
L-glutamine	Fisher Scientific	Cat. # MT25005C1
Minimal Essential Media	Thermo Fisher	Cat. # 11095098
Mini-PROTEAN TGX Gels	Bio-Rad	Cat. # 4561084
Penicillin-Streptomycin	Sigma Aldrich	Cat. # P0781
Plasmocin™ Prophylactic	InvivoGen	Cat. # ant-mpp